

Influence of Battery/Ultracapacitor Energy-Storage Sizing on Battery Lifetime in a Fuel Cell Hybrid Electric Vehicle

Erik Schaltz, *Member, IEEE*, Alireza Khaligh, *Member, IEEE*, and Peter Omand Rasmussen, *Member, IEEE*

Abstract—Combining high-energy-density batteries and high-power-density ultracapacitors in fuel cell hybrid electric vehicles (FCHEVs) results in a high-performance, highly efficient, low-size, and light system. Often, the battery is rated with respect to its energy requirement to reduce its volume and mass. This does not prevent deep discharges of the battery, which are critical to the lifetime of the battery. In this paper, the ratings of the battery and ultracapacitors are investigated. Comparisons of the system volume, the system mass, and the lifetime of the battery due to the rating of the energy storage devices are presented. It is concluded that not only should the energy storage devices of a FCHEV be sized by their power and energy requirements, but the battery lifetime should also be considered. Two energy-management strategies, which sufficiently divide the load power between the fuel cell stack, the battery, and the ultracapacitors, are proposed. A charging strategy, which charges the energy-storage devices due to the conditions of the FCHEV, is also proposed. The analysis provides recommendations on the design of the battery and the ultracapacitor energy-storage systems for FCHEVs.

Index Terms—Battery, energy-management strategy, fuel cell hybrid electric vehicle (FCHEV), ultracapacitor.

I. INTRODUCTION

THE MAIN purposes of the energy-storage devices in fuel cell hybrid electric vehicles (FCHEVs) are to provide the required power to the load during the heating up of the fuel cell stack, to heat up the stack, to supply peak powers to the load to reduce the required power rating of the fuel cell stack, and to capture the braking energy.

The often-used energy storage devices in FCHEVs are batteries, ultracapacitors, or a combination of both. Batteries have a high energy density but limited power density, and ultracapacitors have high power density but limited energy density. Therefore, utilizing both batteries and ultracapacitors provides a compromise of a high-power-density and high-energy-density energy-storage system, resulting in a small, light, and high-performance system [1]–[4].

Manuscript received October 15, 2008; revised May 21, 2009. First published July 21, 2009; current version published October 2, 2009. The review of this paper was coordinated by Prof. A. Miraoui.

E. Schaltz and P. O. Rasmussen are with the Department of Energy Technology, Aalborg University, 9220 Aalborg, Denmark (e-mail: esc@iet.aau.dk; por@iet.aau.dk).

A. Khaligh is with the Energy Harvesting and Renewable Energies Laboratory, Electric Power and Power Electronics Center, Department of Electrical and Computer Engineering, Illinois Institute of Technology, Chicago, IL 60616-3793 USA (e-mail: khaligh@ece.iit.edu).

Color versions of one or more of the figures in this paper are available online at <http://ieeexplore.ieee.org>.

Digital Object Identifier 10.1109/TVT.2009.2027909

This research deals with a low-speed (< 15 km/h) vehicle, which is originally powered by a 6.5-kWh lead-acid battery package. The vehicle is driven by two 2-kW separately excited dc motors. To increase the working radius, the hours of operation, and to avoid the long charging time of the batteries, the battery-powered vehicle is turned into an FCHEV. The fuel cell stack is a high-temperature proton exchange membrane fuel cell, and it is fueled with hydrogen produced by an onboard reformer. Rating the battery in terms of energy does not prevent it from deeper discharges, which might reduce its lifetime. Therefore, sufficient sizing of the battery and the ultracapacitors is an important issue to obtain an appropriate balance between the system volume, the system mass, and the battery lifetime [5]–[7].

This paper has been organized as follows. Section II presents the proposed methodology. The used drive cycle of the FCHEV, the configuration of the propulsion and power systems, and the method used for sizing the power system are described. The modeling of the components of the propulsion and power systems and the energy-management and charging strategies are explained. The method used to compare the system volume, the system mass, and the battery lifetime is also presented. Section III presents the obtained results, where the system volume, the system mass, and the battery lifetime are compared for several energy-storage device ratings. Finally, Section IV provides the conclusion remarks.

II. METHODOLOGY

In this section, the methodology used to obtain the results in Section III is given.

A. Drive Cycles

The torque–speed characteristics of FCHEVs, hybrid vehicles, and electric vehicles versus time are necessary to analyze the behavior of the vehicle. Often, the speed and torque characteristics are obtained in two steps. The first step is to set up models of the vehicles. These models are based on the forces acting on the vehicle, i.e., the forces due to gravity, acceleration, aerodynamic drag, and rolling friction [8]. The second step is to apply a standard drive cycle to the developed models. Since this paper deals with a vehicle used for special applications, there was no standard drive cycle. To obtain information about the speed and torque characteristics, a data logger has been mounted on one of the battery-powered vehicles. The vehicle

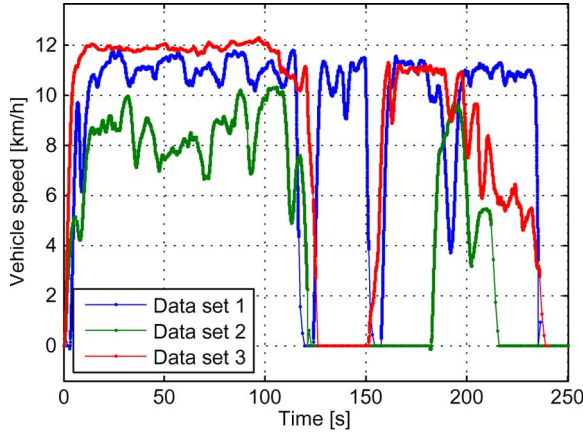


Fig. 1. Vehicle speed for three different driving patterns.

with the data logger was used by a customer during a longer period, and thereby, a realistic drive cycle is obtained. The data logger is used to measure the voltages and currents of the battery and motors of the battery-powered vehicle. A model of the motors is created and utilized to calculate the speed and torque of the motors as a function of time.

In total, $N_{\text{day}} = 24$ days of field measurements were conducted. Fig. 1 demonstrates the vehicle speed for 250 s for three different driving patterns. It is seen that the maximum speed is around 12 km/h. The $N_{\text{day}} = 24$ days of field measurements is used for further analysis.

B. Configuration

Fig. 2 demonstrates the main components of the propulsion and power systems and the power flow in the FCHEV. The fuel cell and energy-storage devices can be connected in various ways [6], [9]–[13], but it is chosen to connect each device to the bus through dc/dc converters. This provides more flexibility to determine the voltage rating of each component [2], [14], [15]. The bus voltage is controlled to a fixed level of $V_{\text{Bus}} = 42$ V.

As shown in Fig. 2, power flows to or from the electric machines (EMs) to a common bus through two inverters (Inv). The energy from the methanol storage (Met) is fed to the bus through a reformer (Ref) and the fuel cell stack (FC). Power is also flowing to or from the battery (Bat) and the ultracapacitors (UC).

The fuel cell and energy-storage devices must not only provide power to the shaft power ($p_{s,L}$ and $p_{s,R}$) but also provide power for the light ($p_{\text{Light}} = 200$ W when speed $\neq 0$), the balance of plant of the fuel cell system ($p_{\text{BoP}} = 0.05 \cdot p_{\text{FC}}$), the fuel cell stack heater, and the auxiliary devices, i.e., vehicle computer, drivers, control panel, etc. ($p_{\text{Aux}} = 50$ W, when either the fuel cell or energy-storage devices are operating). It is assumed that it takes $T_{\text{Heat}} = 6$ min to heat up the fuel cell stack, and the energy required to heat up the stack is $E_{\text{Heat}} = 160$ Wh. Therefore, the power to the heater is $p_{\text{Heat}} = 60E_{\text{Heat}}/T_{\text{Heat}} = 1600$ W.

C. Sizing

The FCHEV is analyzed with a fuel cell stack with a rating of $P_{\text{FC,rat}} = 1000$ W. As a starting point, the battery will have

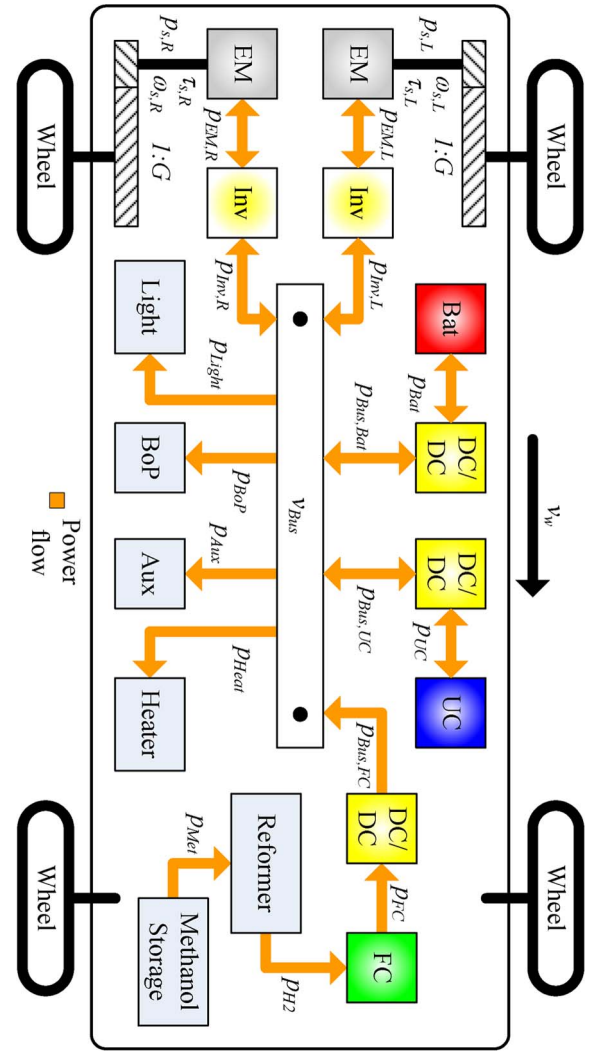


Fig. 2. Configuration, system overview, and power flow of the FCHEV.

a base maximum power and energy rating of $P_{\text{Bat,max,base}} = 5.4$ kW and $E_{\text{Bat,max,base}} = 770$ Wh, respectively. For the ultracapacitors, the base maximum power and energy rating are $P_{\text{UC,max,base}} = 16.8$ kW and $E_{\text{UC,max,base}} = 13.5$ Wh, respectively. With the aforementioned values, the power and energy requirements of the battery and ultracapacitors are fulfilled when the ultracapacitors handle the transient peak powers and the battery takes care of the slower load powers [6]. However, to increase the lifetime of the battery, it will be investigated how the system volume, the system mass, and the battery lifetime will be affected if either the battery or ultracapacitors are overrated.

1) *Overrating of the Battery*: The battery will be overrated with a factor of $a_{\text{or,Bat}} = \{1, 2, 3, 4, 5\}$ relative to the base values. The power and energy rating of the battery are therefore given by

$$P_{\text{Bat,max}} = a_{\text{or,Bat}} \cdot P_{\text{Bat,max,base}} \quad [\text{W}] \quad (1)$$

$$E_{\text{Bat,max}} = a_{\text{or,Bat}} \cdot E_{\text{Bat,max,base}} \quad [\text{Wh}]. \quad (2)$$

When the battery is overrated, it will experience less deep discharge cycles, but the system volume and mass will become bigger.

2) *Overrating of Ultracapacitors*: The ultracapacitors will be overrated with a factor of $a_{or,UC} = \{1, 2, 4, 6, 8, 10\}$. The power and energy rating of the ultracapacitors are therefore

$$P_{UC,max} = a_{or,UC} \cdot P_{UC,max,base} \quad [\text{W}] \quad (3)$$

$$E_{UC,max} = a_{or,UC} \cdot E_{UC,max,base} \quad [\text{Wh}]. \quad (4)$$

The higher energy capacity the ultracapacitors have, the more load power can be delivered from the ultracapacitors instead of from the battery, which will again increase the battery lifetime. However, the system volume and mass will also be increased.

D. Modeling

The two often-used approaches to analyze the power flow of the vehicle are the backward- and forward-looking methods [16]. The backward method starts with the load power and then calculates backward into system, e.g., from the shaft power, the power flowing into the electric machines are calculated, and from the power flowing into the electric machines, the power flowing into the inverters can be calculated. Even though the power actually flows from the inverters through the electric machines to the shafts, when the power is positive, the power flow is calculated in the opposite direction. The forward approach sees the load more as a reference, which can be fulfilled or not, depending on the states and performance of the system. Usually, the backward approach is simpler and faster in comparison with the forward method. However, the forward method is often more realistic. In this paper, the backward approach will be utilized due to its simplicity.

Starting with the angular velocity and shaft torque of the left and right wheels in Fig. 2, i.e., $\omega_{s,L}$, $\tau_{s,L}$, $\omega_{s,R}$, and $\tau_{s,R}$, respectively, the power flow through the rest of the system can be calculated by modeling each of the components.

1) *Electric Machines*: The motors of the FCHEV are of permanent-magnet synchronous-machine type. They are operated with the field-oriented $I_d = 0$ control. The steady-state equations utilized to model the electric machines are

$$\tau_e = B_v \cdot \omega_s + \text{sign}(\omega_s) \cdot \tau_C + \tau_s \quad [\text{Nm}] \quad (5)$$

$$i_q = \frac{2}{3} \frac{\tau_e}{P \lambda_{pm}} \quad [\text{A}] \quad (6)$$

$$v_q = R_s \cdot i_q + \lambda_{pm} \frac{P}{2} \omega_s \quad [\text{V}] \quad (7)$$

$$p_{EM} = \frac{3}{2} v_q \cdot i_q \quad [\text{W}]. \quad (8)$$

τ_e is the electromechanical torque, B_v is the viscous friction coefficient, τ_C is the Coulomb friction, v_q and i_q are the q -axis voltage and current, respectively, R_s is the stator resistance, P is the number of poles, λ_{pm} is the magnet flux linkage, and p_{EM} is the power between the motor and the inverter.

2) *Inverters*: The inverters are assumed to have a constant efficiency of $\eta_{Inv} = 0.95$. The power between the inverter and the bus is therefore

$$p_{Inv} = \begin{cases} \frac{1}{\eta_{Inv}} p_{EM}, & p_{Inv} \geq 0 \\ \eta_{Inv} \cdot p_{EM}, & p_{Inv} < 0 \end{cases} \quad [\text{W}]. \quad (9)$$

3) *Fuel Cell Stack and DC/DC Converter*: It is assumed that the dc/dc converter of the fuel cell stack transfers the fuel cell power (p_{FC}) to the bus with an efficiency of $\eta_{Con,FC} = 0.95$, i.e.,

$$p_{Bus,FC} = \eta_{Con,FC} \cdot p_{FC} \quad [\text{W}]. \quad (10)$$

$p_{Bus,FC}$ is the power between the bus and the fuel cell dc/dc converter. The fuel cell stack is modeled as an open-circuit voltage source $V_{FC,oc}$ with a current-depending series resistance $r_{FC}(i_{FC})$. The resistance $r_{FC}(i_{FC})$ varies with the current drawn from the fuel cell. This way, the characteristic polarization curve of fuel cell is obtained. The fuel cell stack voltage v_{FC} and power p_{FC} are therefore

$$v_{FC} = V_{FC,oc} - r_{FC}(i_{FC}) \cdot i_{FC} \quad [\text{V}] \quad (11)$$

$$P_{FC} = v_{FC} i_{FC} \quad [\text{W}]. \quad (12)$$

i_{FC} is the fuel cell stack current. The fuel cell input power, i.e., the power of the hydrogen p_{H_2} , is given by

$$p_{H_2} = \frac{M_{H_2} N_{FC} LHV_{H_2}}{2F} i_{FC} \quad [\text{W}]. \quad (13)$$

$M_{H_2} = 0.00216$ kg/mol is the hydrogen molar mass, $N_{FC} = 65$ is the number of series connected cells of the fuel cell stack, $LHV_{H_2} = 120.1 \cdot 10^6$ J/kg is the lower heating value of hydrogen, and $F = 96485$ C/mol is Faraday's constant.

4) *Reformer*: The reformer is assumed to have a constant efficiency of $\eta_{Ref} = 0.85$ [17], [18]. The power flowing from the methanol storage is therefore

$$p_{Met} = \frac{1}{\eta_{Ref}} p_{H_2} \quad [\text{W}]. \quad (14)$$

5) *Battery and DC/DC Converter*: The battery is also modeled as an internal voltage source $V_{Bat,int}$ with an internal resistance R_{Bat} . It is again assumed that the dc/dc converter of the battery converts the power between the bus $p_{Bus,Bat}$ and the battery p_{Bat} with an efficiency of $\eta_{Con,Bat} = 0.95$. The equations describing the battery conditions are therefore

$$p_{Bat} = \begin{cases} \frac{1}{\eta_{Con,Bat}} p_{Bus,Bat}, & p_{Bus,Bat} < 0 \\ \eta_{Con,Bat} \cdot p_{Bus,Bat}, & p_{Bus,Bat} \geq 0 \end{cases} \quad [\text{W}] \quad (15)$$

$$R_{Bat} = \frac{V_{Bat,int}^2}{4P_{Bat,max}} \quad [\Omega] \quad (16)$$

$$i_{Bat} = \frac{-V_{Bat,int}}{2R_{Bat}} + \frac{\sqrt{V_{Bat,int}^2 - 4R_{Bat} \cdot p_{Bat}}}{2R_{Bat}} \quad [\text{A}] \quad (17)$$

$$SoC_{Bat} = 1 + \frac{\int (i_{Bat} \cdot V_{Bat,int}) dt}{E_{Bat,max} 3600} \quad [-] \quad (18)$$

$$DoD_{Bat} = 1 - SoC_{Bat} \quad [-]. \quad (19)$$

i_{Bat} , SoC_{Bat} , and DoD_{Bat} are the battery current, the state of charge, and the depth of discharge, respectively. It is seen that when the battery is overrated, i.e., $P_{Bat,max}$ and $E_{Bat,max}$

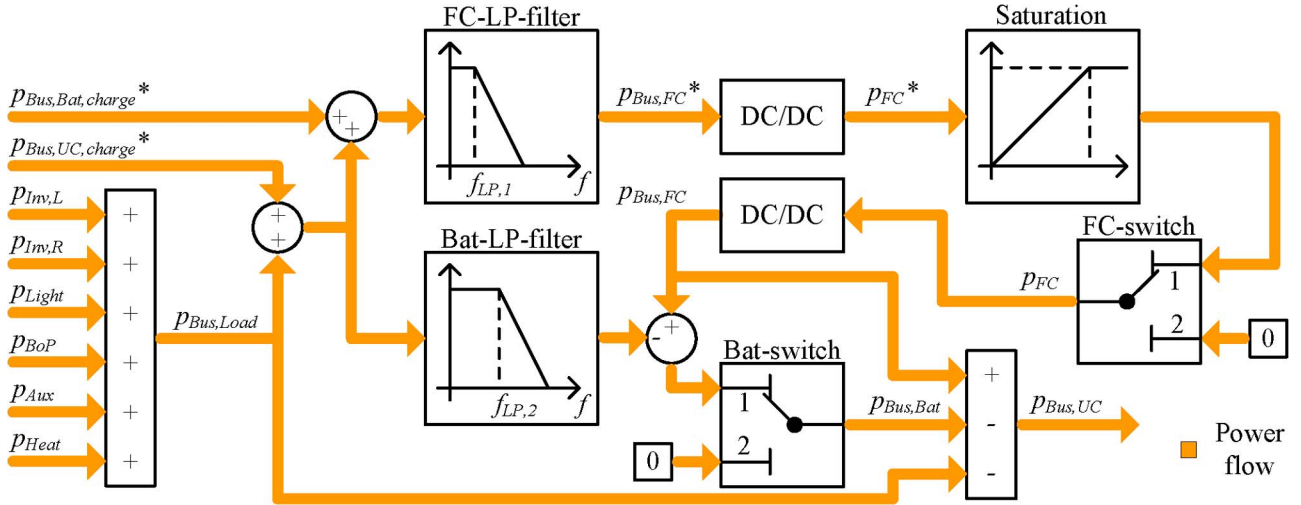


Fig. 3. System-level block diagram of energy-management strategy.

become higher, the battery resistance, the state of charge, and the depth of discharge are directly affected.

6) *Ultracapacitor and DC/DC Converter*: The ultracapacitors are modeled as a series connection of a capacitor C_{UC} and a resistor R_{UC} . Again, it is assumed that the dc/dc converter of the ultracapacitors converts the power between the bus $p_{Bus,UC}$ and the ultracapacitors p_{UC} with an efficiency of $\eta_{Con,UC} = 0.95$. The model of the ultracapacitors is given as

$$p_{UC} = \begin{cases} \frac{1}{\eta_{Con,UC}} p_{Bus,UC}, & p_{Bus,UC} < 0 \\ \eta_{Con,UC} \cdot p_{Bus,UC}, & p_{Bus,UC} \geq 0 \end{cases} \quad [\text{W}] \quad (20)$$

$$R_{UC} = \frac{V_{UC,max}^2}{4P_{UC,max}} \quad [\Omega] \quad (21)$$

$$C_{UC} = \frac{2E_{UC,max}3600}{V_{UC,max}^2} \quad [\text{F}] \quad (22)$$

$$i_{UC} = \frac{-v_{UC,int}}{2R_{UC}} + \frac{\sqrt{v_{UC,int}^2 - 4R_{UC} \cdot p_{UC}}}{2R_{UC}} \quad [\text{A}] \quad (23)$$

$$v_{UC,int} = v_{UC,int}(t=0) + \frac{1}{C_{UC}} \int i_{UC} dt \quad [\text{V}] \quad (24)$$

$$SoC_{UC} = \left(\frac{v_{UC,int}}{V_{UC,max}} \right)^2 \quad [-]. \quad (25)$$

$V_{UC,max}$ and $v_{UC,int}$ are the maximum and the instantaneous internal voltage of the ultracapacitors, respectively. i_{UC} and SoC_{UC} are the current and the state of charge of the ultracapacitors, respectively.

E. Energy-Management Strategies

Sufficient management of the power flow between the fuel cell, the battery, and the ultracapacitors is important to obtain an efficient and high-performance system [4]. Two energy-management strategies are proposed here.

Fig. 3 presents the system-level block diagram of the these strategies. In Fig. 3, “Bat-switch” is used to switch between the two energy-management strategies, i.e., Energy-Management Strategies 1 and 2.

1) *Energy-Management Strategy 1*: The bus load power is defined as

$$p_{Bus,Load} = p_{Aux} + p_{BoP} + p_{Light} + p_{Heat} + p_{Inv,L} + p_{Inv,R} \quad [\text{W}]. \quad (26)$$

In the ideal case, the fuel cell stack should be able to provide power to the loads $p_{Bus,Load}$ and to charge the energy storage devices with their requested charging powers, i.e., $p_{Bus,Bat,charge}^*$ and $p_{Bus,UC,charge}^*$, for the battery and ultracapacitors, respectively. However, due to the low dynamic properties of the reformer, the desired fuel cell bus power contribution $p_{Bus,FC}^*$ is settled by a low-pass filter (Block “FC-LP-filter” in Fig. 3) with bandwidth $f_{LP,1}$. Due to the dc/dc converter, the requested power contribution from the fuel cell is given by

$$p_{FC}^* = \frac{1}{\eta_{FC,Con}} p_{Bus,FC}^* \quad [\text{W}]. \quad (27)$$

To insure that the fuel cell does not deliver more power than its power rating $P_{FC,rat}$ or lower than zero power, the “Saturation” block in Fig. 3 is utilized. If the fuel cell is heating up, it cannot provide power, i.e., $p_{FC} = 0$. In this situation, the switch “FC-switch” in Fig. 3 is therefore in position 2. During normal operation, it is in position 1. The calculation of the fuel cell power p_{FC} may be seen as a simple forward approach, as the fuel cell states are taken into account.

The ultracapacitor base ratings specified in Section II-C were under the assumption that the ultracapacitors are only used for peak powers. When the ultracapacitors only takes care of the peak powers, the “Bat-switch” in Fig. 3 is in position 1. In this situation, the battery contribution is also determined by using a low-pass filter (Block “Bat-LP-filter” in Fig. 3). This filter has a higher bandwidth $f_{LP,2}$ than $f_{LP,1}$ of the fuel cell filter. However, the bandwidth is chosen to be sufficiently low so that the load power due to the short-term accelerations and brakings of the vehicle is fed to the ultracapacitors.

In Fig. 4(a), the fuel cell, battery, and ultracapacitor contributions to the load power are shown for Energy-Management Strategy 1. It is seen that the fuel cell provides the base power,

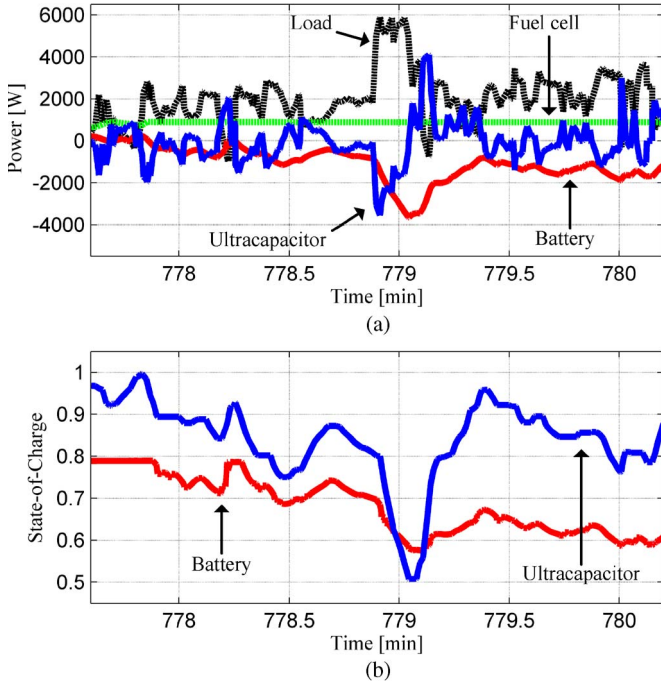


Fig. 4. Results of applying Energy-Management Strategy 1 for overrating factors $a_{or,Bat} = 1$ and $a_{or,UC} = 1$. (a) Bus power. (b) State of charge of energy-storage devices.

the battery delivers the power requirement of low frequency, and the ultracapacitors handle the fast peak powers. Therefore, this way, the ultracapacitors act as a high-pass filter. The results in Fig. 4 are due to overrating factors $a_{or,Bat} = 1$ and $a_{or,UC} = 1$. Therefore, both the battery and the ultracapacitors are discharged to relatively low states, which can also be seen in Fig. 4(b). The battery state of charge changes by approximately 0.2 in the shown time interval.

2) *Energy-Management Strategy 2*: When the ultracapacitors are overrated, it will not be appropriate to only use the ultracapacitors as a high-pass filter, as this not will affect the depth of discharge of the battery, which has influence on the battery lifetime. The ultracapacitors must therefore be operated as an energy source instead of a pure power source. This is obtained by placing the “Bat-switch” in Fig. 3 in position 2. The effect of Energy-Management Strategy 2 is demonstrated in Fig. 5. In this example, the ultracapacitors are overrated with factor $a_{or,U} = 10$, and therefore, they contain sufficient energy so that the battery is not utilized. Therefore, the ultracapacitors handle all of the load power that the fuel cell is not able to deliver. This can be seen in Fig. 5(a). In Fig. 5(b), the state of charge is shown, and it is seen that the battery is not discharged in the presented period. It should also be noticed that the battery is discharged to a higher state-of-charge level than that in Fig. 4(b), where Energy-Management Strategy 1 is used, even though the battery rating is the same for the two examples. However, after some time, the ultracapacitors will be discharged too deep, and one therefore has to utilize the battery again, i.e., placing the “Bat-switch” in position 1, so that the ultracapacitors are again only used for the peak powers.

3) *Selection of Energy Management Strategy*: The minimum state-of-charge level of the ultracapacitors is

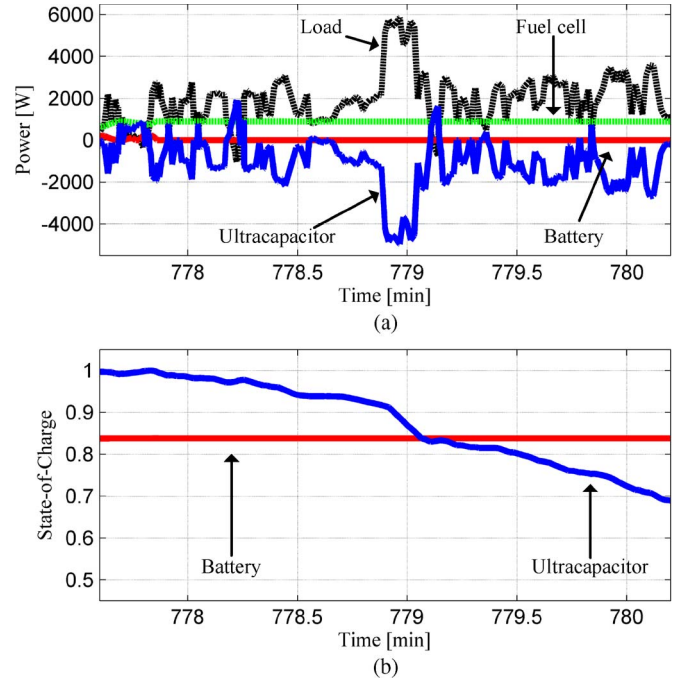


Fig. 5. Results of applying Energy-Management Strategy 2 for overrating factors $a_{or,Bat} = 1$ and $a_{or,UC} = 10$. (a) Bus power. (b) State of charge of energy-storage devices.

$SoC_{UC,min} = 0.25$. This means that when the ultracapacitors are used only for peak powers, the maximum change in energy of the ultracapacitors is

$$E_{UC,peak,max} = (1 - SoC_{UC,min}) \times E_{UC,max,base} [Wh]. \quad (28)$$

When the ultracapacitors are acting as a high-pass filter, the energy level $E_{UC,peak,max}$ has to be available for the peak powers. The critical state-of-charge level that determines if the ultracapacitors should be used as a power or energy source, i.e., Energy-Management Strategy 1 or 2, can therefore be calculated by utilizing (4) and (28)

$$SoC_{UC,crit} = SoC_{UC,min} + \frac{1 - SoC_{UC,min}}{a_{or,UC}} [-]. \quad (29)$$

When the vehicle is inactive, i.e., it is not used by the user, it is chosen to put the “Bat-switch” in position 2. This insures that the ultracapacitors are only charged by the fuel cell and not also by the battery. The selected energy-management strategy is identical to the position of the “Bat-switch” in Fig. 3. Therefore, selecting the energy-management strategy can be determined by a simple expression

```

if (( $SoC_{UC} < SoC_{UC,crit}$ ) OR (Vehicle inactive))
    AND ( $p_{Bus,UC,charge}^* < 0$ )
    Energy-Management Strategy 2
else
    Energy-Management Strategy 1
end
    
```

For both positions of the two switches in Fig. 3, i.e., “Bat-switch” and “FC-switch,” the power between the bus and the dc/dc converter of the ultracapacitors is given by

$$p_{\text{Bus,UC}} = p_{\text{Bus,FC}} - p_{\text{Bus,Load}} - p_{\text{Bus,Bat}} \quad [\text{W}]. \quad (30)$$

F. Charging Strategy

In Fig. 3, it is shown how the load power is divided between the fuel cell stack, the battery, and the ultracapacitors. When the state of charge of the energy-storage devices are below one, the fuel cell charges them, provided there is extra power available. The battery is charged with its 5-h power capacity. Therefore, if ($SoC_{\text{Bat}} < 1$), then

$$P_{\text{Bus,Bat,charge}}^* = \frac{1}{\eta_{\text{Con,Bat}}} \frac{E_{\text{Bat,max}}}{5 \cdot 3600} \quad [\text{W}]. \quad (31)$$

Otherwise

$$P_{\text{Bus,Bat,charge}}^* = 0 \quad [\text{W}]. \quad (32)$$

Due to the health of the ultracapacitors, it is of high importance that they are not overcharged. When the vehicle is used, i.e., active, the ultracapacitors have to capture the braking energy, which means that they should not be fully charged. When the vehicle is active, it is chosen to charge the ultracapacitors to a value, which is presented by (33), where there are two buffers of size equal to $SoC_{\text{UC}} = SoC_{\text{UC,min}}$ and $SoC_{\text{UC}} = 1$, i.e.,

$$SoC_{\text{UC,active}}^* = \frac{1 + SoC_{\text{UC,min}}}{2} \quad [-]. \quad (33)$$

To fully utilize the energy capacity of the ultracapacitors, it is desirable that they are fully charged when the vehicle is inactive. Therefore

$$SoC_{\text{UC,inactive}}^* = 1 \quad [-]. \quad (34)$$

When the ultracapacitors are charged from the fuel cell, the maximum charging power will be the rated fuel cell power $p_{\text{FC, rat}}$. However, while the fuel cell is heating up, the ultracapacitors need to be charged from the battery. In this situation, the battery also has to provide power to the loads. To reduce the stress on the battery, it is, in this situation, therefore decided to charge the ultracapacitors with the 5-h power capacity of the battery.

The proposed energy-management strategies in Fig. 3 suggest that the fuel cell and the battery are operated in a smooth way. However, to insure that the ultracapacitors are not overcharged, it might be necessary to disconnect them when the state of charge approaches $SoC_{\text{UC}} = 1$. Thereby, the fuel cell or battery will be operated in a discontinuous way, which is not desirable. To avoid an abrupt change of power of the fuel cell and the battery, it is chosen to ramp down the ultracapacitor charging power as a function of the state-of-charge level.

TABLE I
SPECIFIC POWER AND ENERGY AND DENSITIES OF THE MAIN COMPONENTS OF THE PROPULSION AND POWER SYSTEMS

	FC	Bat	UC	PE [19]	EM [19]	Ref [20]
Energy density [$\frac{\text{Wh}}{\text{L}}$]	-	71	3.9	-	-	-
Specific energy [$\frac{\text{Wh}}{\text{kg}}$]	-	33	3.2	-	-	-
Power density [$\frac{\text{W}}{\text{L}}$]	62	-	-	11500	3500	1100
Specific power [$\frac{\text{W}}{\text{kg}}$]	131	230	4000	11000	1000	440

A simple algorithm for the requested bus-charging power of the ultracapacitors $p_{\text{Bus,UC,charge}}^*$ is

if ((Vehicle inactive) AND ($SoC_{\text{UC}} < SoC_{\text{UC,inactive}}^*$))
OR ((Vehicle active) AND ($SoC_{\text{UC}} < SoC_{\text{UC,active}}^*$))

if (Fuel cell is heating up)

$$P_{\text{Bus,UC,charge,max}} = \eta_{\text{Con,Bat}} \frac{E_{\text{Bat,max}}}{5 \cdot 3600} \quad [\text{W}] \quad (35)$$

else

$$P_{\text{Bus,UC,charge,max}} = \eta_{\text{Con,FC}} P_{\text{FC, rat}} \quad [\text{W}] \quad (36)$$

end

$$p_{\text{Bus,UC,charge}}^* = P_{\text{Bus,UC,charge,max}} \times \frac{1 - SoC_{\text{UC}}}{1 - SoC_{\text{UC,min}}} \quad [\text{W}] \quad (37)$$

else

$$p_{\text{Bus,UC,charge}}^* = 0 \quad [\text{W}] \quad (38)$$

end.

$P_{\text{Bus,UC,charge,max}}$ is the requested ultracapacitor bus-charging power at minimum state of charge. In (37), it is seen how the charging power is ramped down as the state of charge of the ultracapacitors increases.

G. System Volume and Mass

When the energy-storage devices are oversized, the total system volume and mass will be affected. The system volume and mass are determined by the values in Table I. The system volume and mass are therefore the sum of the volume and mass of the fuel cell stack, battery, ultracapacitors, power electronics (PE), electric machines, and reformer, respectively. The fuel cell stack is a Serenus 166 Air C [24]. It has a nominal power of 920 W, a mass of 7 kg, and a volume of 14.8 L.

H. Battery Lifetime

The lifetime of the battery depends on several parameters, i.e., temperature, the number of peak currents, charge and discharge cycles, etc. [21]. To simplify, only the numbers of the charge and discharge cycles are taken into account.

The cycle to failure for a given depth of discharge of a Trojan deep-cycle gel lead-acid battery can be seen in Fig. 6. This curve has the same shape as a fourth-order polynomial. The

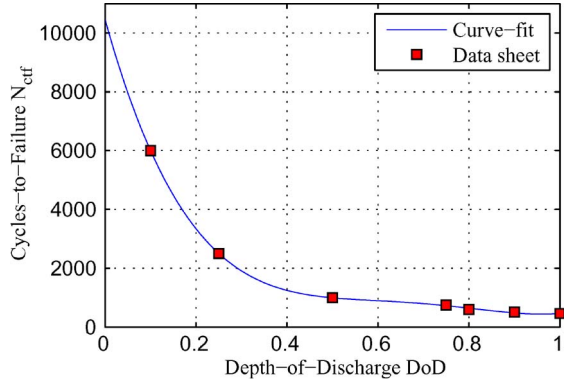


Fig. 6. Cycles to failure versus depth of discharge of a Trojan deep-cycle gel lead-acid battery [23].

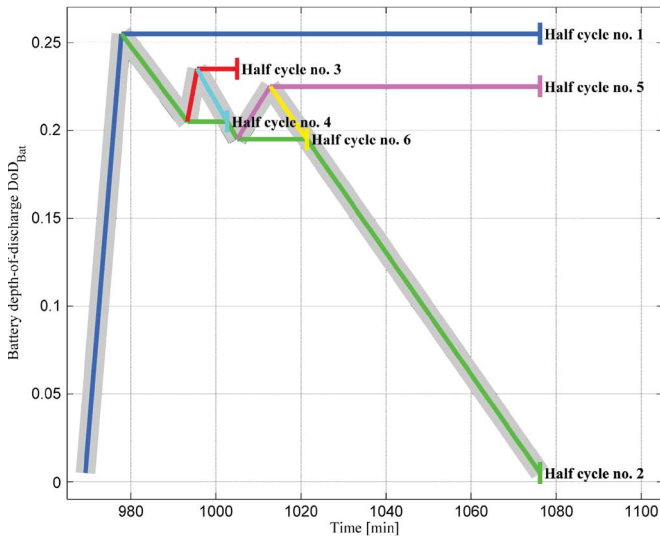


Fig. 7. Battery depth of discharge and calculation of half cycles.

maximum number of cycles versus the depth of discharge of the battery can therefore be expressed as

$$N_{ctf} = -42418 \cdot DoD^4 - 119140 \cdot DoD^3 + 122320 \cdot DoD^2 - 55583 \cdot DoD + 10449 \quad [-]. \quad (39)$$

In Fig. 6, it is seen that the fourth-order approximation in (39) fits the data sheet values. The curve in Fig. 6 shows the maximum number of cycles the battery can handle for one specific depth of discharge. However, during the operation of the battery, it will not be discharged to a specific depth-of-discharge level all the time (unless the energy management strategy decides to do so) but to many different levels. The number of cycles that the battery has experienced for each depth-of-discharge level is calculated by using the rain-flow-counting method [22]. This method simply counts all the cycles that had occurred for each depth-of-discharge level of the battery.

In Fig. 7, it is illustrated how the rain-flow-counting method is applied. The thick gray line is the depth of discharge of the battery, and the thinner colored lines are used to count the number of cycles for one specific depth-of-discharge level. The colored lines are denoted as half cycles. It is seen that each half cycle starts either in a local valley or at a peak. If Fig. 7 is rotated 90° clockwise, the depth-of-discharge curve has a shape

similar to a pagoda roof. By letting a raindrop start at each peak and valley, the half cycle belonging to a specific drop can be obtained by following the drop's path down the roof. However, the drop must stop if one of the following conditions is met.

- 1) It reaches the end of time of the data set, e.g., half cycles 1, 2, and 5.
- 2) It faces a peak/valley that is higher/deeper than its starting peak/valley, e.g., half cycle 3.
- 3) It gets into contact with a previous drop, e.g., half cycles 4 and 6.

The amplitude of each half cycle is the difference between the depth of discharge at its starting and ending points. Half cycles 1 and 2 therefore both have an amplitude of $DoD_{Bat} = 0.25$.

The loss of lifetime of the battery is defined by [21]

$$LoL = \sum_{DoD_{Bat}=0.01}^{DoD_{Bat}=1} \frac{N_{cyc}(DoD_{Bat})}{N_{ctf}(DoD_{Bat})}. \quad (40)$$

N_{cyc} is the number of full cycles with depth-of-discharge amplitude DoD_{Bat} . It may be noticed that to count one full cycle of amplitude DoD_{Bat} , one needs to count two half cycles of amplitude DoD_{Bat} . The end of life of the battery with several depth-of-discharge cycles is reached when $LoL = 1$.

The used drive cycle of this paper is $N_{day} = 24$ days of field measurements. The maximum expected days of operation of the battery before its end of life is therefore given by

$$N_{day,eol} = \frac{N_{day}}{LoL} \quad [\text{days}]. \quad (41)$$

III. RESULTS

The presented model for the FCHEV is analyzed for several overrating factors of the battery and the ultracapacitors. The presented methodology in Section II is applied in modeling the vehicle.

The effect on the battery depth of discharge when either the battery or the ultracapacitors are oversized is shown in Fig. 8. In Fig. 8(a), the number of cycles for a given amplitude of depth of charge is shown for the case when the FCHEV is simulated with the base values of the battery and the ultracapacitors, i.e., for $a_{or,Bat} = 1$ and $a_{or,UC} = 1$. It is seen that the battery experiences many low-amplitude cycles and fewer high-amplitude cycles. In Fig. 8(c), the battery is overrated with factor $a_{or,Bat} = 5$, and it is seen that this significantly improves the discharge level of the battery as the highest depth-of-discharge amplitude is $DoD_{Bat} = 0.1$.

In Fig. 8(b), the ultracapacitors are oversized with factor $a_{or,UC} = 2$. In comparison with Fig. 8(a), it is seen that a significant amount of the low-amplitude energy requirements is handled by the ultracapacitors instead of the battery. However, the number of high discharge states of the battery is not affected for $a_{or,UC} = 2$.

In Fig. 8(d), the ultracapacitors are overrated with factor $a_{or,UC} = 10$. Thereby, they are able to handle a bigger amount of the energy requirement to the loads. This has a positive effect

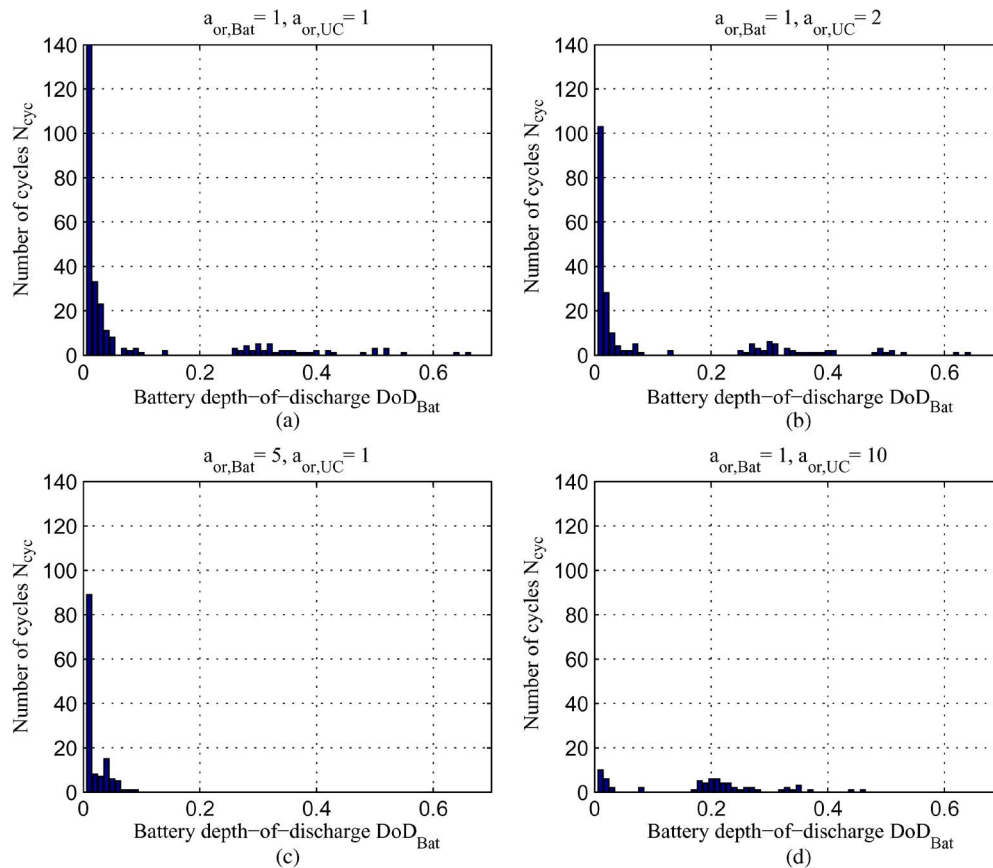


Fig. 8. Number of cycles versus depth of discharge for several overrating factors of the battery and the ultracapacitors. (a) Base values, i.e., $a_{or,Bat} = 1$ and $a_{or,UC} = 1$. (b) Battery has the base value, i.e., $a_{or,Bat} = 1$, and ultracapacitors are overrated with factor $a_{or,UC} = 2$. (c) Battery is overrated with factor $a_{or,Bat} = 5$, and ultracapacitors have the base value, i.e., $a_{or,UC} = 1$. (d) Battery has the base value, i.e., $a_{or,Bat} = 1$, and ultracapacitors are overrated with factor $a_{or,UC} = 10$.

on both the number of cycles with low depth-of-charge amplitudes and the number of cycles with high depth-of-discharge amplitudes. However, for this case, the battery is still needed for big load requirements, i.e., during the heating up of the fuel cell stack.

In Fig. 9, the system volume, the system mass, and the system lifetime of the battery are shown when either the battery or ultracapacitors are overrated.

Oversizing the battery has a significant positive effect on its lifetime, as the battery experiences fewer high depth-of-discharge levels. An overrating factor of $a_{or,Bat} = 3$ increases the days of operation from 375 to 1211 days. However, the system volume and mass are thereby increased by 54% and 90%, respectively. An overrating factor of $a_{or,Bat} = 5$ increases the theoretical battery lifetime by almost 350%, but the system volume is more than doubled, and the system mass is almost tripled. The most appropriate battery rating is therefore a tradeoff between the system volume, the system mass, and the battery lifetime.

Oversizing the ultracapacitors also has a positive effect on the battery lifetime but is not as significant as that for the battery. An overrating factor of $a_{or,UC} = 2$ improves the battery lifetime by 117 days, and no significant effect is seen on the volume and mass of the system. However, for this specific application, it will not be advantageous to oversize the ultracapacitors with more than a factor of $a_{or,UC} = 2$. This can be seen by com-

paring the two cases: when the battery is overrated with factor $a_{or,Bat} = 2$ and when the ultracapacitors are with factor $a_{or,UC} = 4$. The system volume is almost the same, and a significantly better battery lifetime is obtained for $a_{or,Bat} = 2$. Only a small improvement in the system mass is obtained for $a_{or,UC} = 4$.

It may be mentioned that the data sheet of the battery did not contain information regarding the number of cycles with a depth-of-discharge level lower than $DoD = 0.1$. The number of cycles with amplitude lower than $DoD = 0.1$ is therefore based on predictions. When the battery is oversized with factor $a_{Bat} = 5$, all the cycles have amplitudes lower than $DoD = 0.1$, as shown in Fig. 8(c), and the relatively high number of expected days of operation of the battery may therefore not be obtained in practice. However, it is still concluded that overrating the battery will have a positive effect on its lifetime.

IV. CONCLUSION

This paper has dealt with a battery/ultracapacitor FCHEV. The drive cycle utilized for the analysis of the FCHEV is based on more than three weeks of field measurements. The configuration and modeling of the propulsion and power systems of the FCHEV have been presented. Two energy-management strategies and a charging strategy of the energy-storage devices have been proposed. The energy-management strategies divide

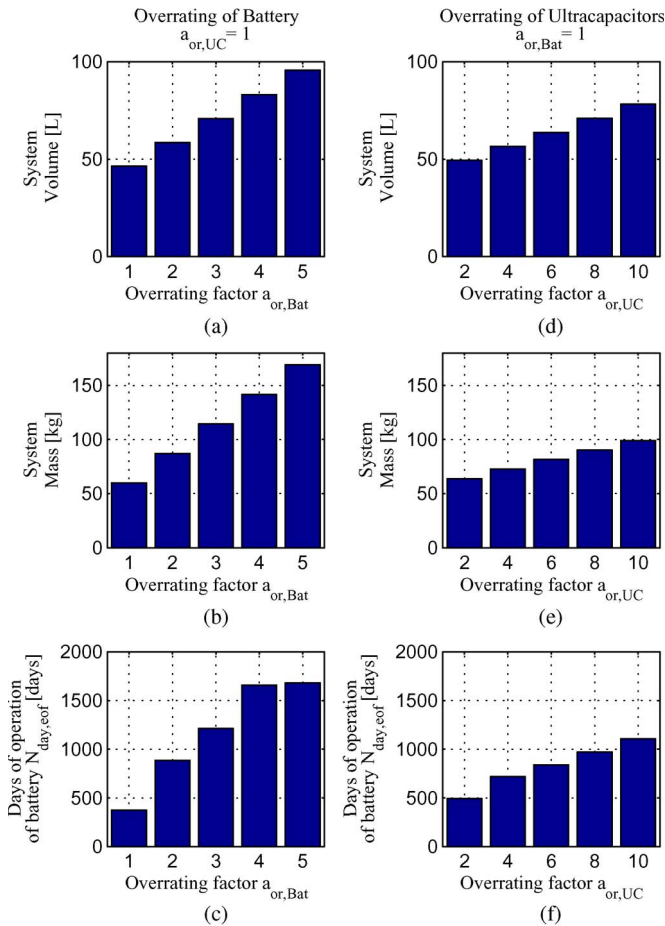


Fig. 9. System volume, system mass, and expected days of operation of the battery when overrating either the battery or the ultracapacitors. (a), (c), and (e) Ultracapacitors have the base value, i.e., $a_{or,UC} = 1$, and the battery is overrated with factor $a_{or,Bat}$. (b), (d), and (f) Battery has the base value, i.e., $a_{or,Bat} = 1$, and the ultracapacitors are overrated with factor $a_{or,UC}$.

the load power between the fuel cell stack, the battery, and the ultracapacitors in such a way that the fuel cell and the battery are operated in a smooth manner. In Energy-Management Strategy 1, the ultracapacitor is operated as a high-pass filter of the load power. In Energy-Management Strategy 2, the ultracapacitor is operated as an energy source, which effectively increases the lifetime of the battery. The charging strategy sufficiently charges the energy-storage devices with respect to the ultracapacitor state of charge and the FCHEV condition.

It has been investigated how the overrating of either the battery or ultracapacitors affects the system volume, the system mass, and the lifetime of the battery. Oversizing the battery or ultracapacitors increases the system volume and mass; however, it also significantly improves the battery lifetime. It has been demonstrated that it is not advantageous to overrate the ultracapacitors more than a factor of $a_{or,UC} = 2$, since better results can be obtained by overrating the battery instead of the ultracapacitors.

The sizing of the battery is a tradeoff between the system volume, the system mass, and the battery lifetime. An overrating factor of $a_{or,Bat} = 3$ increases the battery lifetime by 223%, but the system mass is thereby almost doubled. For an overrating factor of $a_{or,Bat} = 5$, the battery lifetime is

increased by almost 350%, but the system volume is more than doubled, and the system mass is almost tripled. However, for high overrating factors, e.g., $a_{or,Bat} = 5$, all of the depth-of-discharge cycles are of low amplitude, i.e., $DoD < 0.1$, and it is therefore questionable if the high number of battery lifetime is obtainable in practice, due to the uncertainties of low-amplitude cycles. In this specific application, it is therefore recommended that the overrating factor of the battery should be less than $a_{or,Bat} = 5$.

It has been concluded that not only the energy-storage devices of a FCHEV should be sized by their power and energy requirements, but the battery lifetime must be taken into account as well.

The provided analysis give recommendations on the design of battery and ultracapacitor energy-storage systems for the FCHEV.

REFERENCES

- [1] J. Bauman and M. Kazerani, "A comparative study of fuel-cell-battery, fuel-cell-ultracapacitor, and fuel-cell-battery-ultracapacitor vehicles," *IEEE Trans. Veh. Technol.*, vol. 57, no. 2, pp. 760–769, Mar. 2008.
- [2] L. Gao, A. Dougal, and S. Liu, "Power enhancement of an actively controlled battery/ultracapacitor hybrid," *IEEE Trans. Power Electron.*, vol. 20, no. 19, pp. 236–243, Jan. 2005.
- [3] A. C. Baisden and A. Emadi, "ADVISOR-based model of a battery and an ultra-capacitor energy source for hybrid electric vehicles," *IEEE Trans. Veh. Technol.*, vol. 53, no. 1, pp. 199–205, Jan. 2004.
- [4] A. A. Ferreira, J. A. Pomilio, G. Spiazzi, and L. de Araujo Silva, "Energy management fuzzy logic supervisory for electric vehicle power supplies system," *IEEE Trans. Power Electron.*, vol. 23, no. 1, pp. 107–115, Jan. 2008.
- [5] H. Douglas and P. Pillay, "Sizing ultracapacitors for hybrid electric vehicles," in *Proc. 31st Annu. Conf. IECON*, Nov. 2005, pp. 1599–1604.
- [6] E. Schaltz and P. O. Rasmussen, "Design and comparison of propulsion systems for a fuel cell hybrid electric vehicle," in *Conf. Rec. IEEE IAS Annu. Meeting*, Edmonton, AB, Canada, Oct. 2008.
- [7] E. Schaltz, A. Khaligh, and P. O. Rasmussen, "Investigation of battery/ultracapacitor energy storage rating for a fuel cell hybrid electric vehicle," in *Proc. IEEE VPPC*, Harbin, China, Sep. 2008, pp. 1–6.
- [8] M. Ehsani, Y. Gao, S. E. Gay, and A. Emadi, *Modern Electric, Hybrid Electric, and Fuel Cell Vehicles—Fundamentals, Theory, and Design*, 1st ed. Boca Raton, FL: CRC, 2005.
- [9] R. M. Schupbach, J. C. Balda, M. Zolot, and B. Kramer, "Design methodology of a combined battery-ultracapacitor energy storage unit for vehicle power management," in *Proc. IEEE Power Electron. Spec. Conf.*, Jun. 2003, vol. 1, pp. 88–93.
- [10] M. Marchesoni and C. Vacca, "New DC–DC converter for energy storage system interfacing in fuel cell hybrid electric vehicles," *IEEE Trans. Power Electron.*, vol. 22, no. 1, pp. 301–308, Jan. 2007.
- [11] A. Khaligh, A. M. Rahimi, Y. J. Lee, J. Cao, A. Emadi, S. D. Andrews, C. Robinson, and C. Finnerty, "Digital control of an isolated active hybrid fuel cell/Li-ion battery power supply," *IEEE Trans. Veh. Technol.*, vol. 56, no. 6, pp. 3709–3721, Nov. 2007.
- [12] F. Z. Peng, M. Shen, and K. Holland, "Application of Z-source inverter for traction drive of fuel cell battery hybrid electric vehicles," *IEEE Trans. Power Electron.*, vol. 22, no. 3, pp. 1054–1061, May 2007.
- [13] A. Emadi, S. S. Williamson, and A. Khaligh, "Power electronics intensive solutions for advanced electric, hybrid electric, and fuel cell vehicular power systems," *IEEE Trans. Power Electron.*, vol. 21, no. 3, pp. 567–577, May 2006.
- [14] Z. Jiang, L. Gao, and R. A. Dougal, "Flexible multiobjective control of power converter in active hybrid fuel cell/battery power sources," *IEEE Trans. Power Electron.*, vol. 20, no. 1, pp. 244–253, Jan. 2005.
- [15] S. M. Nayeem Hasan and I. Husain, "Power electronic interface with ultracapacitors and motor control for a fuel cell electric vehicle," in *Proc. IEEE VPPC*, Sep. 2005, pp. 815–822.
- [16] D. W. Gao, C. Mi, and A. Emadi, "Modeling and simulation of electric and hybrid vehicles," *Proc. IEEE*, vol. 95, no. 4, pp. 729–745, Apr. 2007.

- [17] J. R. Lattner and M. P. Harold, "Comparison of methanol-based fuel cell processors for PEM fuel cell systems," *J. Power Sources*, vol. 56, no. 1/2, pp. 149–169, Dec. 2005.
- [18] M. Lyubovsky and D. Walsh, "A reforming system for co-generation of hydrogen and mechanical work from methanol," *J. Power Sources*, vol. 162, no. 1, pp. 597–605, Sep. 2006.
- [19] V. Hassani and R. Fessler, *Department of Energy's EE Technical Team Roadmap for Advanced Power Electronics and Electric Machines*, Apr. 2004.
- [20] J. Larminie and J. Lowry, *Electric Vehicle Technology Explained*, 1st ed. New York: Wiley, 2003.
- [21] D. U. Sauer and H. Wenzl, "Comparison of different approaches for lifetime prediction of electrochemical systems—Using lead acid batteries as example," *J. Power Sources*, vol. 176, no. 2, pp. 477–483, Feb. 2008.
- [22] H. Bindner, T. Cronin, P. Lundsager, J. F. Manwell, U. Abdulwahid, and I. Baring-Gould, "Lifetime modelling of lead acid batteries," Risø Nat. Lab., Roskilde, Denmark, Apr. 2005. Risø Rep.
- [23] *Datasheet of Trojan Deep-Cycle Gel Battery*, Trojan Battery Co., Santa Fe Springs, CA, Apr. 2008. [Online]. Available: http://www.trojanbattery.com/pdf/GEL_SS_Web.pdf
- [24] *Datasheet of Serenus 166 Air C Fuel Cell Stack*, Serenergy, Hobro, Denmark, May 2009. [Online]. Available: <http://www.serenergy.com>



Erik Schaltz (M'08) was born in Viborg, Denmark, in 1981. He received the M.S. degree in electrical engineering, with specialization in power electronics, electric machines, and drives, in 2005 from Aalborg University, Aalborg, Denmark, where he is currently working toward the Ph.D. degree with the Department of Energy Technology.

His research interests include analysis, modeling, design, and control of power electronics, electric machines, energy-storage devices, fuel cells, and hybrid electric vehicles.



Alireza Khaligh (S'04–M'06) received the B.S. and M.S. degrees (with highest distinction) from Sharif University of Technology, Tehran, Iran, and the Ph.D. degree from Illinois Institute of Technology (IIT), Chicago, all in electrical engineering.

He was a Postdoctoral Research Associate with the Department of Electrical and Computer Engineering, University of Illinois, Urbana. He is currently an Assistant Professor and the Director of the Energy Harvesting and Renewable Energies Laboratory, Electric Power and Power Electronics Center, Department of Electrical and Computer Engineering, IIT, where he has established courses and curriculum in the area of energy harvesting and renewable-energy sources. He is the author/coauthor of more than 55 journal and conference proceeding papers as well as three books, including *Energy Harvesting: Solar, Wind, and Ocean Energy Conversion Systems* (CRC, 2009), *Energy Sources, Elsevier Power Electronics Handbook* (Elsevier, 2009), and *Integrated Power Electronics Converters and Digital Control* (CRC, 2009). His research interests include the modeling, analysis, design, and control of power electronic converters, hybrid electric and plug-in hybrid electric vehicles, energy scavenging/harvesting from environmental sources, and the design of energy-efficient power supplies for battery-powered portable applications.

Dr. Khaligh is a member of the Vehicle Power and Propulsion Committee, the IEEE Vehicular Technology Society, the IEEE Power Electronics Society, the IEEE Industrial Electronics Society, the IEEE Education Society, and the Society of Automotive Engineers. He is the Conference Chair of the IEEE Chicago Section. He is also an Associate Editor for the IEEE TRANSACTIONS ON VEHICULAR TECHNOLOGY (TVT) and was a Guest editor for the Special Issue of the IEEE TVT on Vehicular Energy Storage Systems. He was also a Guest editor for the Special Section on Energy Harvesting of the IEEE TRANSACTIONS ON INDUSTRIAL ELECTRONICS. He was the recipient of the Distinguished Undergraduate Student Award from Sharif University of Technology, which was jointly presented by the Minister of Science, Research, and Technology and by the President of Sharif University, and the 2009 Armour College of Engineering Excellence in Teaching Award from IIT.



Peter Omand Rasmussen (M'01) was born in Aarhus, Denmark, in 1971. He received the M.Sc. degree in electrical engineering and the Ph.D. degree from Aalborg University, Aalborg, Denmark, in 1995 and 2001, respectively.

In 1998, he joined the Department of Energy Technology, Aalborg University, as an Assistant Professor, where, since 2002, he has been an Associate Professor. His research areas are in the design and control of switched-reluctance and permanent-magnet machines.